



## FRACTURE TOUGHNESS OF CARBON FIBER- EPOXY LAMINATES PROCESSED BY VARTM AND HLUP

### Rita de Cássia Mendonça Sales Contini

Faculdade de Tecnologia de São José dos Campos - Prof. Jessen Vidal  
Instituto Tecnológico de Aeronáutica  
rita.sales@fatec.sp.gov.br

### Silas Rodrigo Gusmão

Faculdade de Tecnologia de São José dos Campos - Prof. Jessen Vidal  
silas.gusmao@gmail.com

### José Maria Fernandes Marlet

Empresa Brasileira de Aeronáutica S.A.  
marlet@embraer.com.br

### Maurício Vicente Donadon

Instituto Tecnológico de Aeronáutica  
donadon@ita.br

**Abstract.** Composite materials are widely used in aeronautic structures due to their high resistance and low density. In aeronautic sector the safety is the most important factor and little damage to the aeronautic structures can be a concern. The most common damage is the delamination, in order words, a failure mode that occurs between the layers due to the fragility of the resin caused by internal failures inserted during the material processing. This paper investigates the interlaminar fracture toughness of carbon fiber-epoxy laminates processed by VARTM (Vacuum Resin Transfer Molding) and HLUP (Hand Lay Up). The processed specimens by VARTM and HLUP were tested using DCB (Double Cantilever Beam) specimens for the Mode I and 4ENF (Four Point End Notched Flexure) specimens for the Mode II delamination to analyze the interlaminar fracture behavior of these composites. The results obtained for each manufacturing technology were compared and conclusions were drawn.

**Keywords:** VARTM, HLUP, DCB, 4ENF, Carbon fiber-epoxy laminates, Delamination.

## 1. INTRODUCTION

Composite materials have significant advantage because of their high strength-to-weight ratio, energy absorption capabilities, flexibility in tailoring directional properties and ability to take complex shapes. Globally, composites are being extensively used for aerospace, defense, transportation and many other industries (Technology Focus, 2010). However, there is a big issue in the composites materials, their high costs of production. Traditional manufacturing process is very expensive, such as the autoclave usage to the prepreg treatment that provides an excellent mechanical property to laminated composite materials (Astrom, 1997).

Therefore, new techniques are being developed to maintain and / or if it's possible increase the composite materials properties, reducing the manufacturing costs. One such technique with low cost is the Vacuum Assisted Resin Transfer Molding (VARTM) (Daniel *et al.*, 2006).

The Vacuum Assisted Resin Transfer Molding (VARTM) is widely used as an alternative to the open mold techniques to produce large components. The VARTM is being widely used by boat and wind turbine blades manufacturers. Significant advances in VARTM research all around the world led to improved quality of this technique. VARTM has been considered promising to replace high-cost fabrication techniques using conventional autoclave in aerospace industry (Matsuzaki *et al.*, 2011).

During the processing of composites obtained by VARTM, the components may exhibit the voids formation in its interior and on the surface. These voids are formed due to potential problems during manufacturing process, such as: bad locking of vacuum bag, resin permeability and low compression between layers of prepreg (Gomes, 2010). The presence of voids in the polymer matrix can be influence directly the shear strength interlaminar compressive and transversal tensile, where the matrix mechanical properties have a greater influence on the composite. Consequently, to increase the reliability of the use of these materials, it is important to know the delamination mechanism and characterize the interlaminar fracture toughness.

In recent years, laminated composites have attracted considerable interest because of the multiple benefits that they offer in the engineering practice. However, it is known that they are susceptible to develop internal failures such as cracks and delamination in the matrix, which can be particularly dangerous for the structural stability leading to premature catastrophic failure. The internal damage are not easily detectable which increases the associated risks. In

Sales, RCM, Gusmão, S.R., Marlet, J.M.F., Donadon, M.V  
Fracture Toughness of Carbon Fiber- Epoxy Laminates Processed by VARTM and HLUP

most real applications, transverse cracks and delamination in the matrix are intrinsically linked and constitute a typical mechanism of damage in composites, especially when the structures are submitted to bending loads (De Moura *et al.* 2010; Shiah *et al.* 2007).

During progressive collapse, front bending following the growth of a main central interwall crack due to delamination in the side wall causes a significant amount of energy absorption. The main central interwall cracks are Mode-I interlaminar crack propagation. Sliding occurs between lamina bundles during front bending, and they dissipate the energy in Mode-II crack propagation (Hadavinia *et al.*, 2009).

Determination of shear strength is a particularly important parameter in the design of these structures. This determination is a difficult task, due to the anisotropic nature of composites and their nonlinear response efforts under shear.

This paper aims at experimental investigation on the interlaminar fracture toughness of carbon/epoxy composite specimens manufactured by VaRTM and HLUP when they are subjected to temperatures equivalent to those that occur in service in different applications, mainly aeronautics. For this purpose, specimens were tested in mode I and mode II loading at different operating temperatures: 25 °C (room temperature) and 80 °C in order to investigate the influence of temperature and the specimens processing type on the toughness  $G_{IC}$  and  $G_{IIC}$  values.

## 2. EXPERIMENTAL PROCEDURE

### 2.1 Specimen preparation

#### 2.1.1 Autoclaving process

The material used to prepare the DCB and 4ENF laminated specimens by autoclaving process was the HexPly® 8552 plain weave carbon fiber AS4 and epoxy resin manufacturing by *Hexcel Composites*.

A rectangular panel (300 mm x 400 mm) was laminated with 24 layers (0°) and a Teflon® film of 0,085 mm thickness inserted in the midplane to represent the initial crack required to the test. The curing process was running at EMBRAER using an autoclave equipment. The panel curing cycle followed the manufacturer's instructions at 180 °C with pressure of 0.70 MPa and vacuum pressure of 0.083 MPa and thermal rate of 0.5-2.7 °C and a cooling rate of 2.7 °C. Then, the panel was demolded and inspected by ultrasonic scanning transmission to observe any discontinuity in the panel.

#### 2.1.2 Vacuum Assisted Resin Transfer Molding

The materials used to prepare the DCB and 4ENF laminated specimens by autoclaving process were: a plain weave carbon fiber HexTow® AS4 and a bicomponent epoxy resin HexFlow® RTM6-2 both manufactured by *Hexcel Composites*.

The plain weave carbon fiber layers was laid down in a plain mold forming a rectangular panel (300 mm x 400 mm) with 24 layers (0°) of dry carbon tissue and a Teflon® film of 0,085 mm thickness inserted in the midplane to represent the initial crack required to the test. A vacuum bagging was placed around the set. After that, it was tested the vacuum bag to observed any air intake.

The components of resin was degassed during 2 h, mixed and heated at 80 °C during 30 min. The mixture was injected by gravity action combined with the vacuum pressure into the bag. After the injection, the set was covered by a thermal blanket heated at 160 °C during 75 min and then the set was brought to a heated oven at 180 °C during 120 min (heating rate: 1 °C/min) to pos cure process. Then, the panel was demolded and inspected by ultrasonic scanning transmission to observe any discontinuity in the panel.

### 2.2 Test procedures

#### 2.2.1 DCB

The specimens' dimensions used to characterize the interlaminar fracture in mode I was conducted in accordance with ASTM D5528-01 (2007) and they are shown in Fig.1. The specified dimensions resulted in a lay-up (0°)<sub>24</sub> named AS4/8552 (HLUP), assuming the thickness of 0.21 mm, and (0°)<sub>24</sub> named AS4/RMT6 (VARTM), assuming the thickness of 0.21 mm. The fiber direction is aligned with the longitudinal direction of the specimen, as shown by Fig. 1.

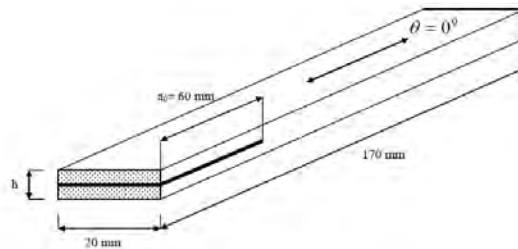


Figure 1. Specimens dimensions used for the interlaminar fracture in mode I characterization ( $h=4.5$  mm to specimens manufactured by HLUP and  $h=5.1$  mm to specimens manufactured by VARTM).

To measure with accuracy the delamination extension, each specimen was painted white. After the ink drying, initial marks were made on the painted surface of 1 mm increments for the first 50 mm of growth from the delamination front and then in 5 mm increments for a further 30 mm.

To the test, it was used alluminium alloy end blocks to apply the load to the specimens. The alluminium blocks were polished, cleaned and bonded with epoxy adhesive to the each side of specimens where there was the Teflon<sup>®</sup> film. The specimen was attached to the grip of a mechanical testing machine *INSTRON 5500R* (Fig. 2). equipped with a load cell of 2 kN (Fig. 3). The load was applied at a rate of 1 mm/min. The tests were conducted at 25 °C and 80 °C, relative humidity of 50 %. A thermal chamber was coupled to the testing machine to carry out the high temperature tests (80 °C).

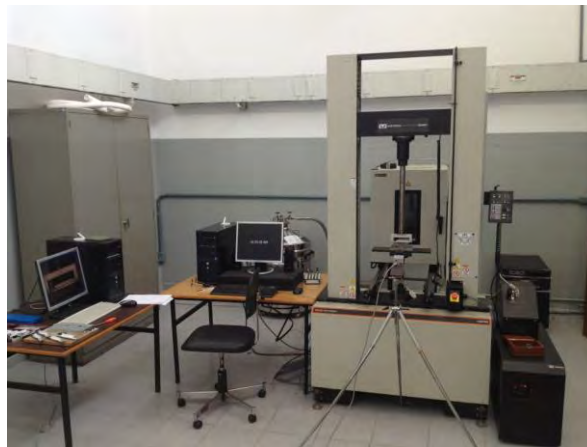


Figure 2. Experimental setup used to characterized Mode I and Mode II interlaminar fracture toughnesses.

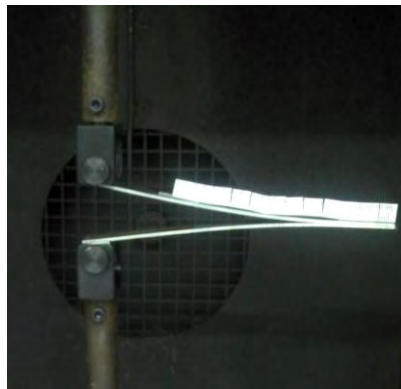


Figure 3. The specimen attached to the mechanical testing machine.

The delamination front extension, in function of load and displacement, was recorded by a crack marker that was pressed every time the crack had been crossed a vertical line marked on specimen improving the observation of the delamination front using a CCD camera positioned on one side of the specimens.

Figure 4 shows the scheme of load used in the DCB specimens, where  $P$  e  $\delta$  are symbols that represent, respectively, the applied load and the transversal displacement in the beginning of load point,  $\alpha$  the delamination extension and  $w$  the specimen width (Cândido *et al.*, 2012a).

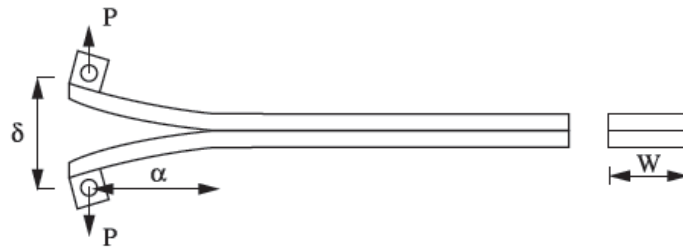


Figure 4. Scheme of specimen load in DCB tests.

The beam theory expression for the strain energy release rate of a double cantilever beam is given as follows Eq.(1)(ASTM D5528-01, 2007):

$$G_I = \frac{3P\delta}{2wa} \quad (1)$$

where  $P$  = load,  $d$  = load point displacement,  $w$  = specimen width and  $a$  = delamination length.

In practice, this expression will overestimate  $G_I$  because the beam is not perfectly built-in (that is, rotation may occur at the delamination front). One way of correcting for this rotation is to treat the DCB as if it contained a slightly longer delamination,  $a + |\Delta|$ , where  $\Delta$  may be determined experimentally by generating a least squares plot of the cubic root of compliance,  $C^{1/3}$ , as a function of delamination length. The compliance,  $C$ , is the ratio of the load point displacement to the applied load,  $\delta/P$  and  $F_c$  is the correction factor associated to larger displacements. The values used to generate this plot should be the load and displacements corresponding to the visually observed delamination onset on the edge and all the propagation values. The expression to compute the Mode I interlaminar fracture toughness including the corrections for large displacements and rotations is given by (ASTM D5528-01, 2007):

$$G_I = \frac{3P\delta F_c}{2w(a + |\Delta|)} \quad (2)$$

### 2.2.2 4ENF

The specimens dimensions used to characterized the interlaminar fracture in mode II were chosen in accordance with a procedure developed by researchers of Material Engineering Research Laboratory Ltd (MERL)(Martin *et al.*, 1999) and they are shown in Fig.5. the specified dimensions resulted in a lay-up  $(0^\circ)_{24}$  named AS4/8552 (HLUP), assuming the thickness of 0.21 mm, and  $(0^\circ)_{24}$  named AS4/RMT6 (VARTM), assuming the thickness of 0.21 mm. The fiber direction is aligned with the longitudinal direction of the specimen (Fig. 5).

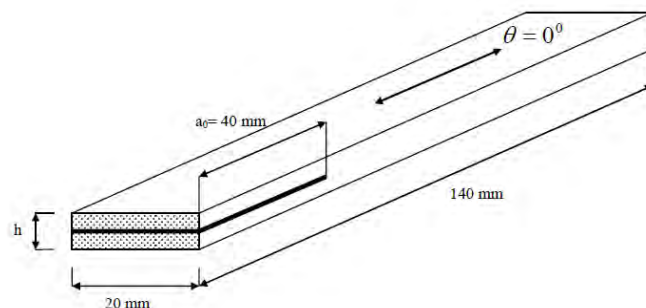


Figure 5. Specimens dimensions used for the interlaminar fracture in mode II characterization ( $h=4.5$  mm to specimens manufactured by HLUP and  $h=5.1$  mm to specimens manufactured by VARTM).

To measure with accuracy the delamination extension, each specimen was painted white laterally. After the ink drying, initial marks were made on the painted surface of 1 mm increments for the first 50 mm of growth from the delamination front and then in 5mm increments for a further 30 mm.

The specimen was set up in a apparatus experimental and this set was connected to the mechanical testing machine *INSTRON 5500R* equipped with a load cell of 30 kN (Fig. 6). The load was applied at a rate of 1 mm/min. The tests

were conducted at 25 °C and 80 °C, relative humidity of 50 %. A thermal chamber was coupled to the testing machine to carry out the high temperature tests (80 °C).

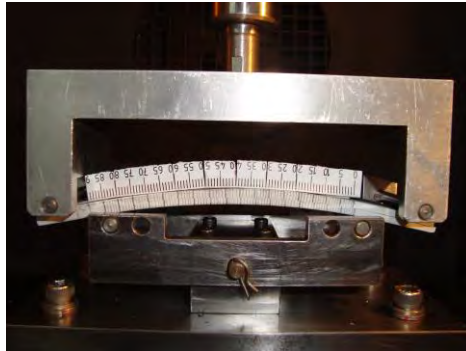


Figure 6. The specimen set up used for mode II interlaminar fracture toughness characterization.

The delamination front extension, in function of load and displacement, was recorded by a crack marker every that the crack had been crossed a vertical line marked on specimen improving the observation of the delamination front using a CCD camera positioned on one side of the specimens.

Figure 7 shows the scheme of load used in the 4ENF specimens, where  $P$  e  $\delta$  are symbols that represent, respectively, the applied load and the vertical point displacement.

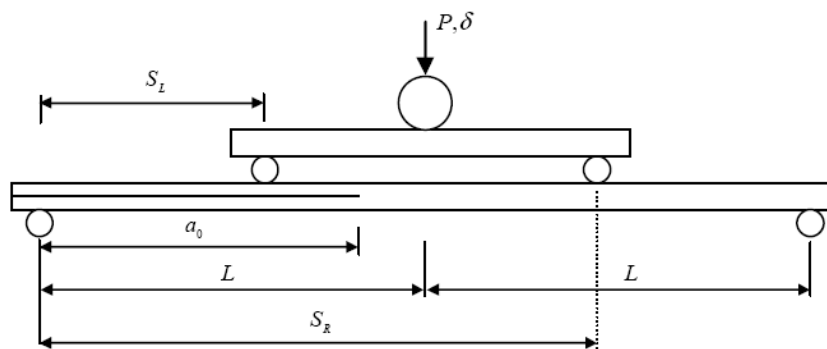


Figure 7. Scheme of specimen loading apparatus used in the 4ENF tests (Cândido *et al.*, 2013b).

The data reduction for 4ENF test were carried out in accordance with Martin *et al.*, 1999. The mode II interlaminar fracture toughness  $G_{IIc}$  was calculated as follows Eq.(3):

$$G_{II} = \frac{P^2 m}{2w} \quad (3)$$

where  $w$  is the specimen width and  $P$  is the applied load. The constant  $m$  is the slope of the best fit straight line defined by the compliance against delamination length curve.

### 3. RESULTS AND DISCUSSION

#### 3.1 Double cantilever beam tests

Figures 8 and 9 show the results obtained for five specimens manufactured by HLUP process and submitted to the DCB tests at 25 °C and 80 °C.

In the Fig. 8a and Fig.9a it is observed that the load increases linearly until it reaches the maximum load where the crack starts, which is followed by a gradual decrease due to crack propagation. It is also observed some „stick–slip“ behavior, in all cases, due to local variations of the material systems, particularly on the first increment, where there is an artificially high toughness induced by the region rich in resin ahead the crack tip (Martin and Davidson, 1999; Siddiqui *et al.*, 2007). Others variations can influence this phenomenon such as fiber-rich region along the longitudinal direction, misalignment of fibers and void as well as fiber bridging or fibers bundles (Kim *et al.*, 1992).

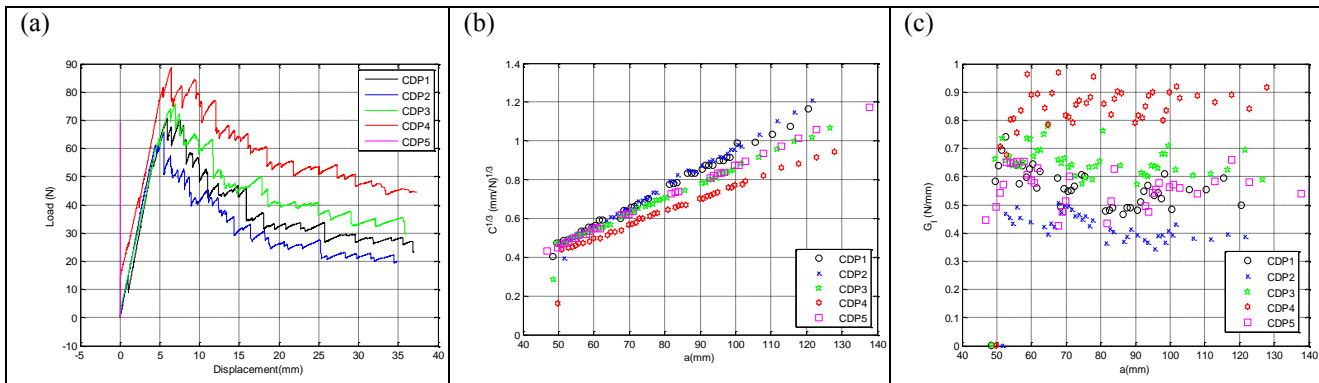


Figure 8 . Mode I Results: (a) Curve P versus  $\delta$  (b)  $C^{1/3}$  versus delamination extension  $a$  e (c) Curve  $G_I$  versus delamination extension  $a$  of specimen manufactured by HLUP process and analyzed at 25 °C.

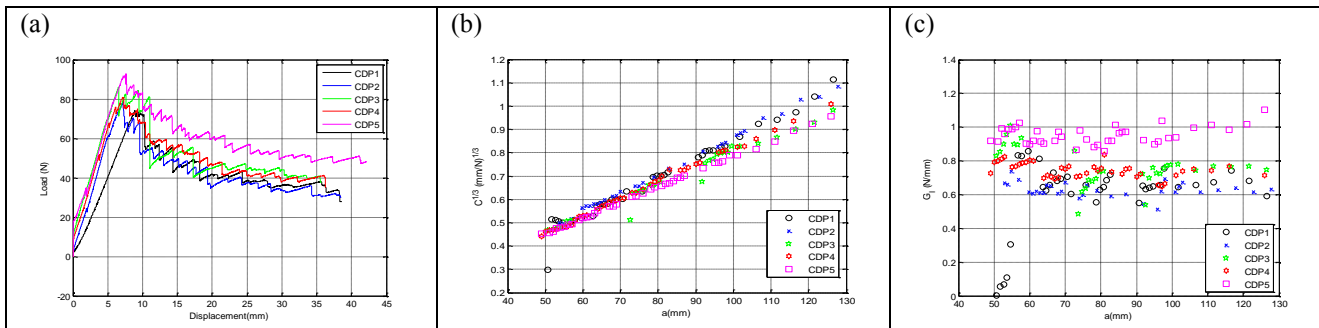


Figure 9 . Mode I Results: (a) Curve P versus  $\delta$  (b)  $C^{1/3}$  versus delamination extension  $a$  e (c) Curve  $G_I$  versus delamination extension  $a$  of specimen manufactured by HLUP process and analyzed at 80 °C.

Figures 10 and 11 show the results obtained of five specimens manufactured by VARTM process and submitted to the DCB tests at 25 °C and 80 °C.

In the Fig. 10a and Fig.11a it is observed the same behavior in the results compared that obtained in specimens processed by HLUP process, but the „stick-slip“ phenomenon is more pronounced in the specimens manufactured by VARTM due to the quantity of voids presents in the material inherent to the manufacturing process.

$G_I$  values variation (Fig. 11c and Fig. 12c) decrease according to the crack propagation mainly in the specimens tested at 80 °C. This decrease has been observed because of a slight decrease in stiffness along the specimen with the test temperature increasing (Coronado *et al*, 2012).

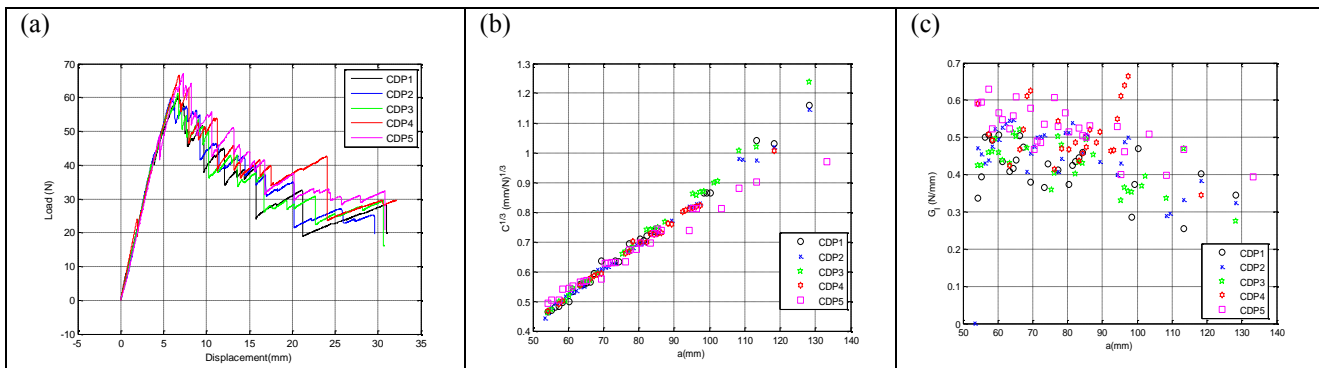


Figure 10 . Mode I Results: (a) Curve P versus  $\delta$  (b)  $C^{1/3}$  versus delamination extension  $a$  e (c) Curve  $G_I$  versus delamination extension  $a$  of specimen manufactured by VARTM process and analyzed at 25 °C.

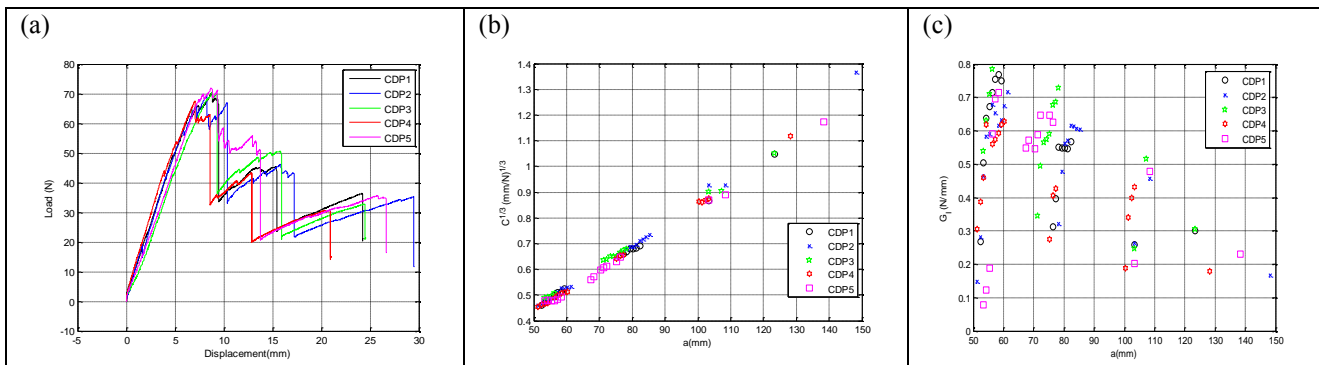


Figure 11 . Mode I Results: (a) Curve  $P$  versus  $\delta$  (b)  $C^{1/3}$  versus delamination extension  $a$  e (c) Curve  $G_I$  versus delamination extension  $a$  of specimen manufactured by VARTM process and analyzed at 80 °C.

A summary of  $G_I$  average value of the strain energy release rate at crack propagation is showed in Table 1. It is observed that the  $G_I$  values are higher with increasing of test temperature. According to the Coronado *et al.*, 2012, in general, the analyzed composite shows more brittle behavior at low temperatures and a significant increase in the ductility of the matrix as the temperature increases.

Comparing the  $G_I$  values (Table 1) for the manufacturing processes, it can be observed that those specimens manufactured by VARTM have a lower  $G_I$  values than those manufactured by HLUP which showed the opposite trend due to less void content in these materials which is favored by the higher layers compression due to the high pressure in autoclave during the manufacturing process.

It is possible to compare the  $G_I$  values to the same manufacturing process in different temperatures. It can be noticed that to the HLUP process the  $G_I$  value at 80 °C is 21 % higher than at 25 °C. The same behavior can be observed in specimens processed by VARTM, the  $G_I$  value at 80 °C is 8 % higher than at 25 °C. According to Hutapea and Yuan, 1999, high temperature increases both  $G_I$  values at test temperature near  $T_g$  due to the strongest bond between the fibers and the matrix.

Table 1. Mode I Interlaminar Fracture Toughness values for both manufacturing process.

Manufacturing Process	Temperature (°C)	Mean $G_I$ (N/mm)	Standard deviation $G_I$ (N/mm)
HLUP	25	0.6118	0.1748
HLUP	80	0.7382	0.1389
VARTM	25	0.4648	0.0478
VARTM	80	0.5022	0.0508

### 3.2 Four-point end-notched flexure tests

Figures 12 and 13 show the results obtained of five specimens manufactured by HLUP process and submitted to the 4ENF tests at 25 °C and 80 °C.

It can be noticed that the load increases linearly until it reaches the maximum load where the crack subtly initiated and the „stick-slip“ appears. Once the lamination had grown a small amount, the load was observed to remain constant with the delamination length and with a minor evidence the „stick-slip“ phenomenon (Martin and Davidson, 1999; Siddiqui *et al.*, 2007).

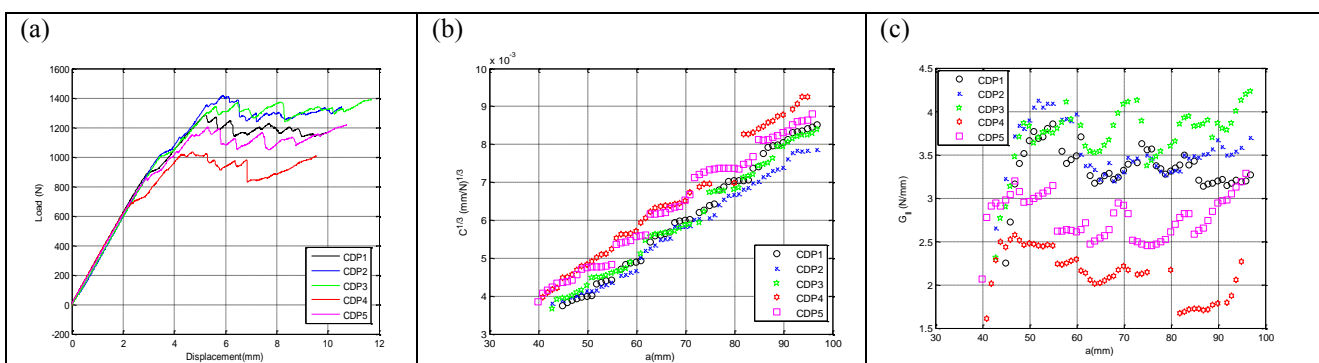


Figure 12 . Mode II Results: (a) Curve P versus  $\delta$  (b)  $C^{1/3}$  versus delamination extension  $a$  e (c) Curve  $G_I$  versus delamination extension  $a$  of specimen manufactured by HLUP process and analyzed at 25 °C.

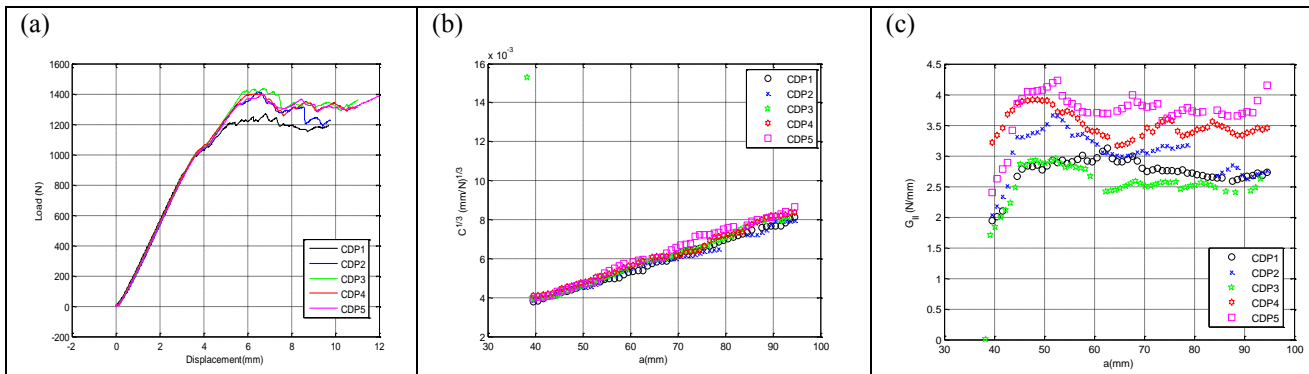


Figure 13 . Mode II Results: (a) Curve P versus  $\delta$  (b)  $C^{1/3}$  versus delamination extension  $a$  e (c) Curve  $G_I$  versus delamination extension  $a$  of specimen manufactured by HLUP process and analyzed at 80 °C.

Figures 14 and 15 show the results obtained of five specimens manufactured by VARTM process and submitted to the 4ENF tests at 25 °C and 80 °C.

It can be noticed that the „stick-slip” behavior is less pronounced than that observed in the specimens manufactured by HLUP. This phenomenon may be explained due to a significant increase in the ductility of the matrix as the temperature increases.

It is also interesting that  $G_{II}$  appears to decrease to a constant value with increasing amounts of delamination advance.

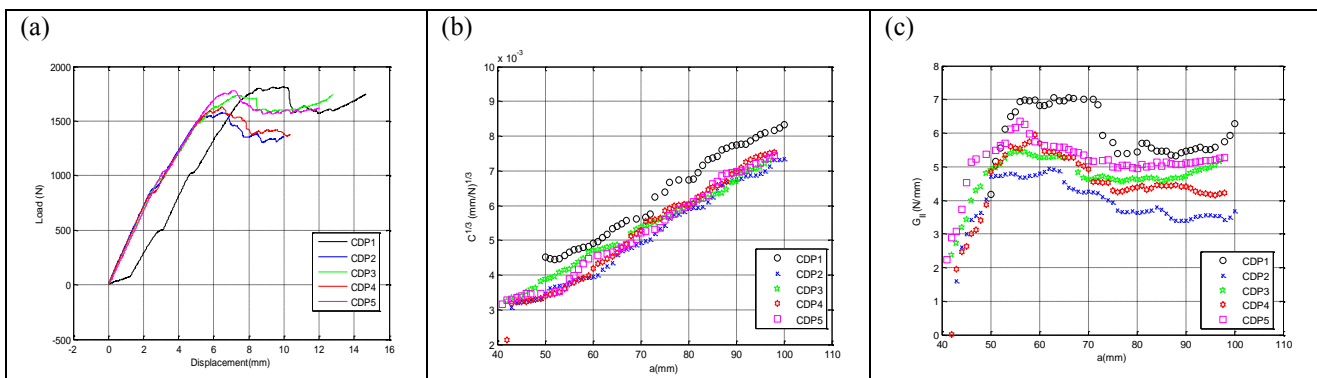


Figure 14 . Mode II Results: (a) Curve P versus  $\delta$  (b)  $C^{1/3}$  versus delamination extension  $a$  e (c) Curve  $G_I$  versus delamination extension  $a$  of specimen manufactured by VARTM process and analyzed at 25 °C.

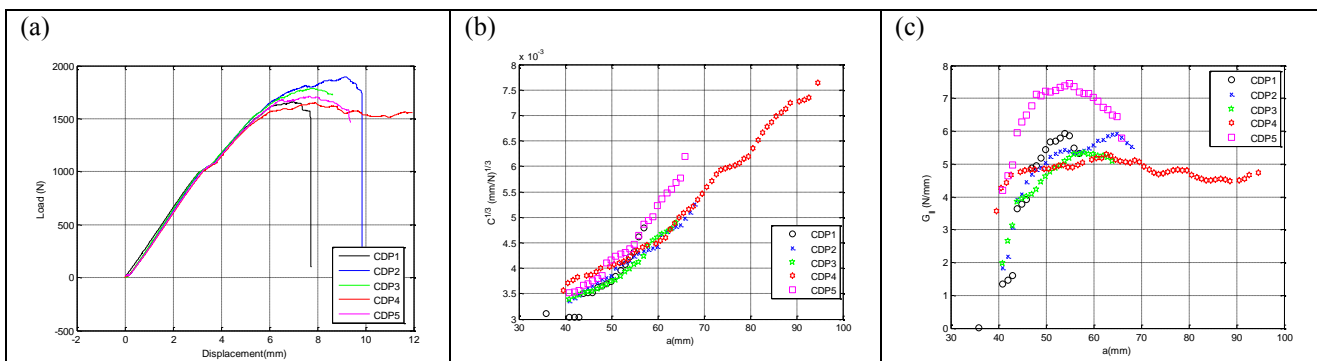


Figure 15 . Mode II Results: (a) Curve P versus  $\delta$  (b)  $C^{1/3}$  versus delamination extension  $a$  e (c) Curve  $G_I$  versus delamination extension  $a$  of specimen manufactured by VARTM process and analyzed at 80 °C.

Table 2 summarizes the results obtained for the interlaminar fracture toughness in Mode II to the specimens manufactured by HLUP and VARTM, respectively.

Table 2. Mode II Interlaminar Fracture Toughness values for both manufacturing process.

Manufacturing Process	Temperature (°C)	Mean $G_{II}$ (N/mm)	Standard deviation $G_{II}$ (N/mm)
HLUP	25	3.103	0.6496
HLUP	80	3.110	0.5075
VARTM	25	4.871	0.7853
VARTM	80	5.030	0.9352

$G_{II}$  values in Table 2 show that specimens manufactured by VARTM have a higher  $G_{II}$  values than those manufactured by HLUP.

It is possible to compare the  $G_{II}$  values to the same manufacturing process in different testing temperatures. It can be noticed that to the HLUP process the  $G_{II}$  value at 80 °C is 0.22 % higher than at 25 °C. The same behavior can be observed in specimens processed by VARTM, the  $G_{II}$  value at 80 °C is 3.26 % higher than at 25 °C. These values suggest that there are a strongest bond between fibers and matrix promoted to the higher temperature.

Comparing the values obtained to the Mode-I (Table 1) and Mode-II (Table 2) for both manufacturing process, it is observed the  $G_I$  values are smaller than  $G_{II}$ .

$G_{II}$  value was calculated as total fracture toughness energy at the maximum load sustained by the material as the delamination extended. Mode-II interlaminar fracture toughness energy values were naturally higher than mode-I values as expected due to loading conditions that fibers can resist the crack growth better since they are perpendicular to crack opening (Saidpour *et al*, 2003).

A possible explanation for this unique phenomenon may be the semi-contact situation because of friction between the upper and lower beams of the specimen before Mode II delamination onset, when bending moment slid the upper and lower beams and forced some parts into a semi-contact situation; this can be viewed as a reversal of the delamination growth (similar to „crack closure“). In contrast, the semi-contact situation does not exist in the DCB specimen before Mode I delamination onset, when a tensile force separates the upper and lower beams and keeps them in a complete non-contact situation (Wang *et al*, 2012).

#### 4. CONCLUSIONS

Mode I and II interlaminar fracture toughness and delamination crack growth behavior at 25 °C and 80 °C were investigated for the carbon/epoxy composite specimens manufactured by HLUP and VARTM process. The results are summarized as follows:

- 1- In the DCB tests it was observed that the specimens manufactured by HLUP have higher  $G_I$  values than specimens manufactured by VARTM, in both temperatures, that can be caused because of void content in the matrix.
- 2- The specimens manufactured by VARTM have higher  $G_{II}$  values indicating that they are more resistant under in-plane shear deformation mode.
- 3- In HLUP and VARTM process, it was noticed that the high temperature the  $G_I$  and  $G_{II}$  values are higher than the room temperature maybe because the high temperature increased both values at test temperature near  $T_g$  due to the strongest bond between the fibers and the matrix.
- 4- The values obtained to the Mode-II is higher than Mode-I values for both manufacturing process indicating that the high value is due to the semi-contact situation because of friction between the upper and lower beams of the specimens promoting a reversal of the delamination growth (similar to „crack closure“).

#### 5. REFERENCES

- ASTM D 5528 – 01. *Standard Test Method for Mode I Interlaminar Fracture Toughness of Unidirectional Fiber-Reinforced Polymer Matrix Composites*. West Conshohocken, 2007.
- Astrom, BT. *Manufacturing of polymer composites*. London: Chapman and Hall; 1997.
- Cândido, G.M., Rezende, M.C., Donadon, M.V., Almeida, S.F.M., 2012a. “Fractografia de Compósito Estrutural Aeronáutico Submetido à Caracterização de Tenacidade à Fratura Interlaminar em Modo I”. *Polímeros*, Vol. 22, n. 1, p. 41-53.
- Cândido, G.M., Rezende, M.C., Donadon, M.V., Almeida, S.F.M., 2013b. “Fractografia de Compósito Estrutural Aeronáutico Submetido ao Ensaio de Tenacidade à Fratura Interlaminar em Modo II”. *Polímeros*, Ahead of Print. <http://dx.doi.org/10.4322/polimeros.2013.008>.

Sales, RCM, Gusmão, S.R., Marlet, J.M.F., Donadon, M.V  
Fracture Toughness of Carbon Fiber- Epoxy Laminates Processed by VARTM and HLUP

- Coronado, P. , Argüelles, A., Viña, J., Mollón, V. , Viña, I., 2012. “Influence of temperature on a carbon–fibre epoxy composite subjected to static and fatigue loading under mode-I delamination”. *International Journal of Solids and Structures*, Vol. 49, p. 2934–2940.
- Daniel I.M., Ishai O. Engineering mechanics of composite materials. 2<sup>nd</sup> ed. New York: Oxford University Press; 2006.
- De Moura, M.F.S.F., Campilho, R.D.S.G., Amaro A.M., Reis P.N.B.,2010. “Interlaminar and intralaminar fracture characterization of composites under mode I loading”. *Composite Structures*, Vol.92, p.144–149.
- Gomes, P.P, 2010. *Caracterização e simulação do fluxo de resina do processo de VARTM na obtenção de compósitos de carbono/ epóxi*. Master Dissertation, ITA, São José dos Campos.
- Hadavinia, H., Ghasemnejad, H., 2009. “Effects of Mode-I and Mode-II interlaminar fracture toughness on the energy absorption of CFRP twill/weave composite box sections”. *Composite Structures*, Vol.89, p. 303–314.
- Hutapea, P. and Yuan, F.G., 1999. “The effect of thermal aging on the Mode-I interlaminar fracture behavior of a high-temperature IM7/LaRC-RP46 composite”. *Composites Science and Technology*, Vol. 59, p. 1271-1286.
- Kim, J.K., Baillie, C., Poh J and Mai, Y.W. 1992. “Fracture toughness of CFRP with modified epoxy matrices”. *Composites Science and Technology*. Vol. 43, p. 283-297.
- Martin, R. H. and Davidson, B. D., 1999. “Mode II fracture toughness evaluation using four point bend, end notched flexure test”. *Plastics, Rubber and Composites*, Vol. 28 n. 8, p. 401.
- Matsuzaki,R., Kobayashi, S., Todoroki, A., Mizutani, Y., 2011. “Full-field monitoring of resin flow using an area-sensor array in a VARTM process”, *Composites: Part A*, Vol. 42, p.550–559.
- Saidpour, H., Barikani, M. and Sezen, M., 2003. “Mode-II Interlaminar Fracture Toughness of Carbon/Epoxy Laminates”. *Iranian Polymer Journal*, Vol 12, n.5, p.389-400.
- Shiah, Y.C., Chen, Y.H., Kuo, W.S., 2007. “Analysis for the interlaminar stresses of thin layered composites subjected to thermal loads”. *Composites Science and Technology*, Vol. 67, p.2485–2492.
- Siddiqui, N.A, Woo, R.S;C., Kim, J.K., Leung C.K.Y., Munir A., 2007. “Mode I Interlaminar Fracture behaviour and mechanical properties of CFRPs with Nanoclay filled epoxy matrix”. *Composites Part A: Applied Science and Manufacturing*, Vol. 38, n. 2, p. 449-460.
- Technology Focus, 2010. *Bulletin of Defense Research and Development Organization*, Vol. 18, n.1, p.1-12.
- Wang, D., Ye, L. , Tang, Y., Lu, Y., 2012. “ Monitoring of delamination onset and growth during Mode I and Mode II interlaminar fracture tests using guided waves”. *Composites Science and Technology*, Vol. 72, p.145–151.

## 6. RESPONSIBILITY NOTICE

The authors are the only responsible for the printed material included in this paper.